European Review for Medical and Pharmacological Sciences 2020; 24: 6311-6322

MiR-140-5p targets BCL2L1 to promote cardiomyocyte apoptosis

M.-Y. SUN[1], L.-P. LI[2]

[1]Department of Clinical Laboratory, Jining No. 1 People's Hospital, Jining, China
[2]Department of Cardiology, Jining No. 1 People's Hospital, Jining, China

Abstract. – OBJECTIVE: Recovery of blood flow after ischemic cardiomyopathy can lead to aggravation of myocardial injury. This is very detrimental to the patient's prognosis. The purpose of this study was to investigate the effects and mechanisms of microRNA-140-5p (miR-140-5p) on myocardial ischemia-reperfusion injury (IRI).

MATERIALS AND MODELS: We made the myocardial IRI model in rats and detected the expression of miR-140-5p. Anta-miR-140-5p was administered intravenously in the tail of rats. Then, we used 2, 3, 5-triphenyl tetrazolium chloride staining, cardiac function test, and histological experiment to observe the chan in myocardial infarct size, cardiac functi cardiomyocyte apoptosis in rats. In *in v* periments, we induced the damage of H9c by hypoxia/reoxygenation (H/R) model and tected the effects of miR-140-5p on the proli ation ability and apoptosis leve H9c2 cell TargetScan database was u dict the binding target of miR-140-5 we fied the effect of miR-140-5p on t rget th gh Dual-Luciferase reporter a

RESULTS: MiR-140-5p ly myocardial tissue of rat a-miR-140-5p can reduce myo ial infa a, improve cardiac function reduce the f myocardial cells ap in rats. The ession of miR-140-5 H ced H9c2 cells was higher than t in the l group. MiR-140-5p inhibito as found to te the proliferation an crease the apop level of H9c2 cells, w miR-140-5p mimic w s the opposite. The etScan stem predicts the presence of g sit r miR 40-5p and B-cell lymphoma-like (BCL2 The Dual-Luciferase reporte found t miR-140-5p can bind CL2L1 ro its degradation. In addition, inhi BCL2L1 was found to promot optosis 9c2 cells.

C LUSIONS: In myocardial IRI, miR-140-5p tar and promotes its degradation, th by ind g myocardial apoptosis.

Words:
140-5p, Myocardial ischemia-reperfusion injury, .

Introductio

Acute ocar farction (AMI) is one of the diseases with hi rbidity and mortality wor It is mainly acterized by myoc ischemic necrosis caused by coronary arobstruction[1]. eperfusion therapy is the bafor improvin e prognosis of AMI patients. ever, reperf n itself increases irreversible d to the cardium and coronary circulatio leading to an increase in the infarction area. This pathological change is called yocardial ischemia-reperfusion injury (IRI)[2]. l[3] found that when patients with AMI d ne accept reperfusion therapy, the area of myocardial infarction accounted for 70% of the ischemic danger area, and only accepting reperfusion therapy could reduce the area of myocardial infarction to 40%. When patients get both reperfusion therapy and myocardial protection therapy that can prevent myocardial IRI, the area of myocardial infarction will be significantly reduced to 5%. Therefore, to restore effective reperfusion of myocardium while adopting myocardial protection measures that can effectively prevent myocardial IRI will be the key to reduce the mortality and complication rate of AMI patients.

The mechanisms of myocardial IRI are diverse, such as free radical damage, calcium overload, oxidative stress, and myocardial energy metabolism disorders[4]. A variety of factors can jointly lead to the apoptosis of myocardial cells and irreversible damage to the myocardium. Cardiovascular disease and microRNA (miRNA) are closely related. MiRNAs have 20-24 nt in length and do not encode proteins. The biological functional diversity of miRNA is its distinctive feature[5]. MiRNAs can promote mRNA degradation through complementary pairing. In addition, there are many miRNA species, and 1048 species have been found. Among total human genes, miRNAs account for

Corresponding Author: Linping Li, MM; e-mail: llp0522@163.com

only 2%, of which 20-30% are related to gene regulation[6]. Although the proportion of miRNAs is low, they play a strong regulatory role, especially in cell growth, cell proliferation, and apoptosis. MiRNAs play an increasingly important role in the occurrence and development of cardiovascular disease[7]. The knockout of some miRNAs often triggers myocardial remodeling and even heart failure[6]. There are many types of miRNA specific to cardiomyocytes. According to statistics, there are more than 800 types, including miR-1, miR-133, miR-24, miR-126, miR-145, miR-30, miR-132, and miR-122. When myocardial ischemia occurs, miRNAs will change significantly, especially in symptoms, such as hypoxia[8].

MiR-140-5p belongs to the members of the miRNA family and is a common mature miRNA produced by miR-140 precursors. MiR-140-5p can regulate cell growth, tissue differentiation, organ development, and the occurrence of various cancers[9]. MiR-140-5p can act as a tumor suppressor on multiple different target genes and inhibit the invasion of tongue squamous carcinoma cells[10]. In addition, miR-140-5p can inhibit the proliferation and metastasis of hepatoma carc[illegible] cells, and can also participate in the f[illegible] of myelin sheath and the occurrence of ob[illegible][11]. However, the effect of miR-140 on myocardia[illegible] was rarely studied. Therefore, we made the [illegible] rat model and observed the role of miRNA-14[illegible] 5p in myocardial IRI, laying a[illegible]n for the subsequent research on the [illegible]hani[illegible]f myocardial IRI.

Materia[illegible]nd M[illegible]s

Animals

Sprague D[illegible]y (2[illegible]g, male) was purchased and rai[illegible]d at the Jin[illegible] 1 People's Hospital An[illegible] Center. The ra[illegible]e placed in an SPF ba[illegible] facilit[illegible] (12 hours of [illegible]lternating light, 20-2[illegible] 40-70% [illegible]ative humidity) and fed with cle[illegible]ter an[illegible]t food. [illegible]is study was approved by the [illegible]thics C[illegible]mittee of Jining No. 1 P[illegible]ple's [illegible]l An[illegible] Center.

My[illegible]rdial IR[illegible]odel

T[illegible]ats were anesthetized with 1.55% sodium pe[illegible] mg/kg) based on body weight. [illegible] rats were then fixed on the operating table in [illegible]pine position. The rat trachea was cut open a[illegible]nected to a small animal ventilator (CWE SAR[illegible]0, Orange, CA, USA). The small animal ventilator is set to a ventilation frequency of 60-80 beats per minute, a tidal volume of 2[illegible] a breathing ratio of 1.5:1. After the [illegible] the [illegible]terior cardiac region of the rat wa[illegible] infected by iodophor, we used a sterile scal[illegible]ut from the rat's left chest and bluntly separate[illegible]ue until the heart was exposed. Aft[illegible]he peric[illegible] wa[illegible] gently cut with a scalpel[illegible]left anterior[illegible] ding branch of the cor[illegible]y arter[illegible] of the ra[illegible] ligated with a sterile[illegible]re. Th[illegible]evation of the ST segment of the e[illegible]ar[illegible]am at[illegible]time indicates that th[illegible]oro[illegible]od flo[illegible]s successfully bloc[illegible] After li[illegible]g[illegible]for[illegible] minutes, the ligature[illegible]loosened for[illegible]. We, then, took bloo[illegible] rat femoral [illegible]ery and used cardiac [illegible]soun[illegible]easure cardiac function. Finally, we collected [illegible]art of the rats. Rats in the [illegible]antagomir (a[illegible]ontrol (Con) group a[illegible] anta-miR-140-5p group were injected [illegible] 200 μL of [illegible]ta-Con and anta-miR-140-5p [illegible]he tail vein[illegible]e days before modeling, re-[illegible]tively. Anta[illegible]n and anta-miR-140-5p were c[illegible]cted in [illegible]ghai GenePharma (Shanghai, Chi[illegible]

Cardiac Function Test

[illegible]rs after the rat's coronary arteries were [illegible]per[illegible]ed, we used echocardiography to measure the ejection fraction (EF), short-axis contraction fraction (FS), and stroke output (SV) of the rat. EF, FS and SV can reflect the function of [illegible]at hearts. A decrease in their value indicates a decrease in cardiac function.

2, 3, 5-Triphenyl Tetrazolium Chloride (TTC) Staining

Rat hearts were washed twice with physiological saline and frozen in a -20 °C refrigerator. The hearts were then transected into 2 mm thick slices perpendicular to the long axis. Heart slices were then stained in 2% TTC staining solution (Sigma-Aldrich, St. Louis, MO, USA) at 37°C. 4% paraformaldehyde was used to fix the heart slices. Image J 1.51k (National Institutes of Health, Bethesda, MA, USA) was used to calculate the infarct area.

Histology and Hematoxylin-Eosin (HE) Staining

Rat hearts were washed twice with normal saline and fixed in 4% paraformaldehyde for 24 hours. Myocardial tissue was washed with phosphate buffered saline (PBS). Myocardial tissue was dehydrated in ethanol solutions of different

concentrations. The dehydrated myocardial tissue was put into xylene and paraffin solution in order, and finally made into paraffin blocks. We then cut the paraffin block into 5 μm thick paraffin sections using a microtome (LEICA RM2235, Koln, Germany). Paraffin sections were placed in a 37°C incubator for 24 hours, and then, stored at room temperature. Before HE staining, paraffin sections were baked in a 55°C incubator for 1 hour. Paraffin sections were then dewaxed in xylene and hydrated in ethanol. The sections were then soaked in hematoxylin staining solution (Sigma-Aldrich, St. Louis, MO, USA) for 3 minutes. After differentiation with hydrochloric acid alcohol, the sections were stained with cytoplasm in eosin staining solution (Sigma-Aldrich, St. Louis, MO, USA). Finally, the sections were dehydrated and sealed with neutral gum. A high-power optical microscope (LEICA, Koln, Germany) is used to observe the morphology of myocardial tissue.

Immunohistochemical (IHC) Staining

After dewaxing and hydration, the sections were placed in citrate buffer and heated to 95°C for 20 minutes. After the temperat[ure] of citrate buffer was naturally cooled t[o] temperature, we took the sections and inc[ubated] the myocardial tissue with 3% H_2O_2 for 3[0] nutes. We, then, washed the sections with P[BS] and incubated the myocardial tissue with 10[%] goat serum for 1 hour. After[,] the remaining water on the sectio[ns] we in[cubated] the myocardial tissue with p[rimary] ant[ibody] dilution (caspase-3, Abcam, [Cambridge], caspase-8, Abcam, C[ambridge], USA) at 4°C overnight. The[next] day, [after] washing the sections with PB[S] we incubate[d] sections with the second[ary] body dilution [of] the IHC staining kit (ZSGB-Bio, Shanghai, China) for 1 hour and w[ashed] the sec[tions] with PBS. Finally, we use th[e] coloring solution [of] IHC staining kit for [the] development. A high-power optical micr[oscope] (LEICA, Koln, Germany) was used to [observe] the [results] of [IHC] staining.

RNA Isolation and Quantitative Reverse Transcription-Polymerase Chain [Reaction] (qRT-PCR)

Before extracting RNA from m[yo]cardial tissue and H9c2 cells, we immersed [consumables], such as Eppendorf (EP; Hamburg, Ger[many]) tubes and pipette tips in diethyl pyro[carbonate] (DEPC) wa[ter] (Beyotime, Shanghai, [China]) for 12 [hours] to remove RNase from t[he] consumables. My[ocar]dial tissue was cut a[nd] placed i[n] Eppendorf (EP) tubes containing 1 [mL] TRI[zol] reagent (Invitrogen, Carlsbad, C[A], USA). [Homogenizer] was used to grind myoc[ardi]al tissue. [Then] 1 mL chloroform was then ad[ded] to the EP tu[be after] mixing, the EP tu[be] placed in a ce[ntri]fuge (12000 rpm, 10 [minutes], [at] and the supernatant was collected. 500 μL of [isopropyl] ethanol was added to t[he] tubes and m[ixed]. Spin column tubes w[ere] then used to collect the RNA from the solu[tion]. 700 μL of B[uffer] RWT and 500 μL of RPE [were] used to wa[sh] the RNA, respectively. Finally, [we] used RNase-[free] water to dissolve the RNA i[n the] Spin tub[e] and collected the RNA solution in [the] tubes. The RNA extraction method in H9c2 cells is similar to the above. RNA was first reversed into complementary deoxyribonucleic acid (cDNA). The RT system was 2 μL total RNA + 1 μL 2.5U/μU PolyA Polymerase + 1 μL RTase Mix + 5 μL 5 × Reaction buffer + 16 μL RNase-free water (Invitrogen, Carlsbad, CA, USA). SYBR Green Master Mix (Invitrogen, Carlsbad, CA, USA) was used to amplify cDNA. The primer sequences were shown in Table I. U6 expression was used as a control for miR-140-5p, and glyceraldehyde 3-phosphate dehydrogenase (GAPDH) expression was used as a control for mRNA. The expression amount of RNA was represented by $2^{-\Delta\Delta CT}$.

Detection of Lactate Dehydrogenase (LDH) in Serum

After collecting the blood of rats, we obtained the serum by centrifugation (3000 rpm, 5 minutes, 4°C) and stored it in a -80°C refrigerator. The

Table I. R[NA] [p]rimer [s]equences.

Name	Sense sequences (5′-3′)	Anti-sense sequences (5′-3′)
mi[R-140-5p]	ACATGAGCTATCGACGCATGTC	TCGGCTACTGAGGCGCAAA
	GGAACGCGAAGAAAAGTG	ATTTTGAATCCACGGAGGT
[Cas]pase8	CACATCCCGCAGAAGAAG	GATCCCGCCGACTGATA
[BC]L2L1	ACCCCTCTTCCCTCCAG	CCTCAGCCAACTCTACGC
	GCTTCGGCAGCACATATACTAAAAT	CGCTTCACGAATTTGCGTGTCAT
G[APDH]	ATGGCTACAGCAACAGGGT	TTATGGGGTCTGGGATGG

standards were diluted to different concentrations (1.25, 2.5, 5, 10, 20, 40 IU/mL). Then, 50 µL of the test sample and standard were added to a 96-well plate. After the 96-well plate was incubated in a 37°C incubator for 30 minutes, we added 50 µL of enzyme-labeled reagent to each well and made it incubated for another 30 minutes. Finally, 50 µL of developer was added to each well and we used a microplate reader (Molecular Devices, Santa Clara Valley, MD, USA) to detect the absorbance of each well at 450 nm.

Cell Culture

Rat myocardial cell line, H9c2 cells, were used in this study. We used 445 mL of Dulbecco's Modified Eagle's Medium (DMEM; Gibco, Rockville, MD, USA), 50 ml of fetal bovine serum (FBS; Gibco, Rockville, MD, USA), and 5 mL of double-antibody (Gibco, Rockville, MD, USA) configured as a complete medium to culture H9c2 cells. Cells were cultured in a 37°C incubator and all cell experiments were performed in a sterile cell clean bench.

Procedure of Hypoxia/Reoxygenation (H/R) Model

H9c2 cells were seeded in Petri dishes. After the cell density reached 80%, we replaced the culture medium with hypoxia solution for 12 hours. Then, 99.9% nitrogen was passed into the incubator. The volume fraction of oxygen was controlled to less than 1% for 4 hours. Then, we restored the normal culture conditions and the cells continue to culture for 3 hours.

Transfection

NC mimic, miR-140-5p mimic, NC inhibitor, miR-140-5p inhibitor and siRNA-BCL2L1-sense: AUGAAUCUACA and siRNA-BCL2L1-antisense: UGCUAUACGAGCAGUU.

Cell Counting Kit-8 (CCK8) Assay

H9c2 cells were seeded in 96-well plates. After the cell growth density reached 50%, we treated the cells differently and added 10 µL of CCK8 reagent (Yifeixue, Nanjing, China) to each well. The cells were then incubated for 2 hours. Finally, we used a microplate reader to detect the absorbance of each well at 450 nm.

Immunofluorescence (IF) Staining

H9c2 cells were seeded in 24-well plates. After the cell growth density reached 50%, we treated cells differently. We then washed the cells with PBS. Cells were immersed in 4% paraformaldehyde for 20 minutes and then immersed them in 0.5% Triton-100 for 15 minutes. After washing the cells with PBS, 10% goat serum was used to block non-specific antigens for 30 minutes. We, then, incubated the cells at 4°C overnight using primary antibody dilution (Caspase-3, Abcam, Cambridge, MA, USA; caAbcam, Cambridge, MA, USA). The next day, we washed away the excess primary antibody with PBS and incubated the cells with the secondary antibody dilution (Abcam, Cambridge, MA, USA) for 1 hour. Then, we stained the nucleus with DAPI (Sigma-Aldrich, St. Louis, MO, USA). Finally, we used a fluorescence microscope (LEICA, Koln, Germany) to observe the staining results.

MiRNA Target Prediction and Dual-Luciferase Reporter Assay

We searched the TargetScan database (http://www.targetscan.org/vert_72/) for target genes that could bind to miR-140-5p. After obtaining the possible target gene of miR-140-5p, we verified it by Dual-Luciferase reporter assay. H9c2 cells were seeded in large petri dishes. After the cell growth density reached 85%, we collected H9c2 cells and washed them with PBS. The cells were divided into WT-BCL2L1 + NC mimic group, WT-BCL2L1 + miR-140-5p mimic group, MUT-BCL2L1 + NC mimic group and MUT-BCL2L1 + miR-140-5p mimic group. After the transfected cells were cultured in an incubator for 48 hours, the cells were added to a 96-well plate and 75 µL of Dual-Glo Luciferase Reagent (Millipore, Billerica, MA, USA) was added to each

well. We, then, used a fluorophotometer (Thermo Fisher Scientific, Waltham, MA, USA) to detect the Luciferase content.

Flow Cytometry

We collected H9c2 cells and washed them with PBS. After centrifugation (1000 rpm, 5 minutes), 5 μL of AnnexinV-FICT (Sigma-Aldrich, St. Louis, MO, USA) was added to the centrifuge tubes and mixed. After 10 minutes, 1 μL of 100 μg/μL PI staining solution was added to a centrifuge tube and incubated for 5 minutes. Finally, 400 μL of each tube was detected by flow cytometry.

Statistical Analysis

All data in this study were entered into the EXCEL form for storage and analysis using Statistical Product and Service Solutions (SPSS) 20.0 statistical software (IBM Corp., Armonk, NY, USA). The results of the analysis are expressed as mean ± standard deviation (SD). The differences between the two groups were analyzed by using the Student's *t*-test. Comparison between multiple groups was done using One-way ANOVA test followed by post-hoc test (Least Significant Difference). All experiments were repeated more than 3 times. $p<0.05$ indicates that the difference is statistically significant.

Results

MiR-140-5p Was High[ly] Expressed in Myocardial Tissue [of] Rat Anta-MiR-140-5p Can Reduce Myocardial IRI

The rats were divided into Sham group, IRI group, IRI + anta-Con group and IRI + anta-miR-140-5p group. The expression of miR-140-5p in the myocardial tissue of the four groups of rats was detected and the expression of miR-140-5p in the IRI and IRI + anta-Con groups was higher than that in the Sham group and the IRI + anta-miR-140-5p group (Figure 1A). We measured the area of myocardial infarction in rats by the TTC staining. The area of myocardial infarction in IRI and IRI + anta-Con group was higher than that in Sham group and IRI + anta-miR-140-5p group (Figure 1B). In addition, we measured the concentration of LDH in rats. Compared with the Sham group, the LDH the concentration of the rats in the IRI group and the IRI + anta-Con group was significantly increased. Anta-miR-140-5p can reduce the concentration of LDH (Figure 1C). Myocardial IRI also caused a decrease in cardiac function in rats, manifested as a decrease in EF (Figure 1D), FS (Figure 1E), and SV (Figure 1F), while anta-miR-140-5p could partially restore cardiac function in rats. The results of RT-PCR found that anta-miR-140-5p can reduce the caspase3/8 (Figure 1G). We examined the pathological changes of myocardial tissue by HE staining (Figure 1H). The cardiomyocytes of the rats in the IRI group and the IRI + anta-Con group were significantly disturbed and there was inflammatory cell infiltration among the cardiomyocytes, while cardiomyocytes of the rats in the IRI + anta-miR-140-5p group were significantly improved. We detected the expression of apoptosis-related molecule caspase3/8 in rat myocardial tissue by IHC staining and the results showed that the apoptosis level of myocardial cells in rats was higher than that in the Sham group and anta-miR-140-5p could reduce the level of apoptosis (Figure 1H).

MiR-140-5p Was Highly Expressed in H/R-Induced H9c2 Cells and MiR-140-5p Inhibitor Can Reduce H/R-Induced Cell Damage

The proliferation level of H9c2 cells treated with H/R was detected by CCK-8 assay. The proliferation level of cells treated with H/R decreased compared to the Control group, indicating that H/R can successfully induce H9c2 cell damage (Figure 2A). Then, miR-140-5p was found to be highly expressed in H9c2 cells of the H/R group (Figure 2B). NC mimic, miR-140-5p mimic, NC inhibitor and miR-140-5p inhibitor were constructed to detect the effects of miR-140-5p on H9c2 cells. RT-PCR was used to verify the transfection efficiency of miR-140-5p mimic and miR-140-5p inhibitor (Figure 2C). Flow cytometry was used to detect the cell apoptosis rate and it was found that miR-140-5p inhibitor can inhibit the apoptosis of H9c2 cells, while miR-140-5p mimic is the opposite (Figure 2D). In addition, we detected the expressions of caspase3/8 mRNA and protein in H9c2 cells using RT-PCR (Figure 2E) and IF staining (Figure 2F, G), respectively. The results also demonstrated the anti-apoptotic effect of miR-140-5p on H9c2 cells.

MiR-140-5p Binds BCL2L1 and Induces its Degradation

TargetScan database was used to predict the targets of miR-140-5p. In rats, miR-140-5p was predicted to have a conserved binding site to BCL2L1 (Figure 3A). Therefore, we used the

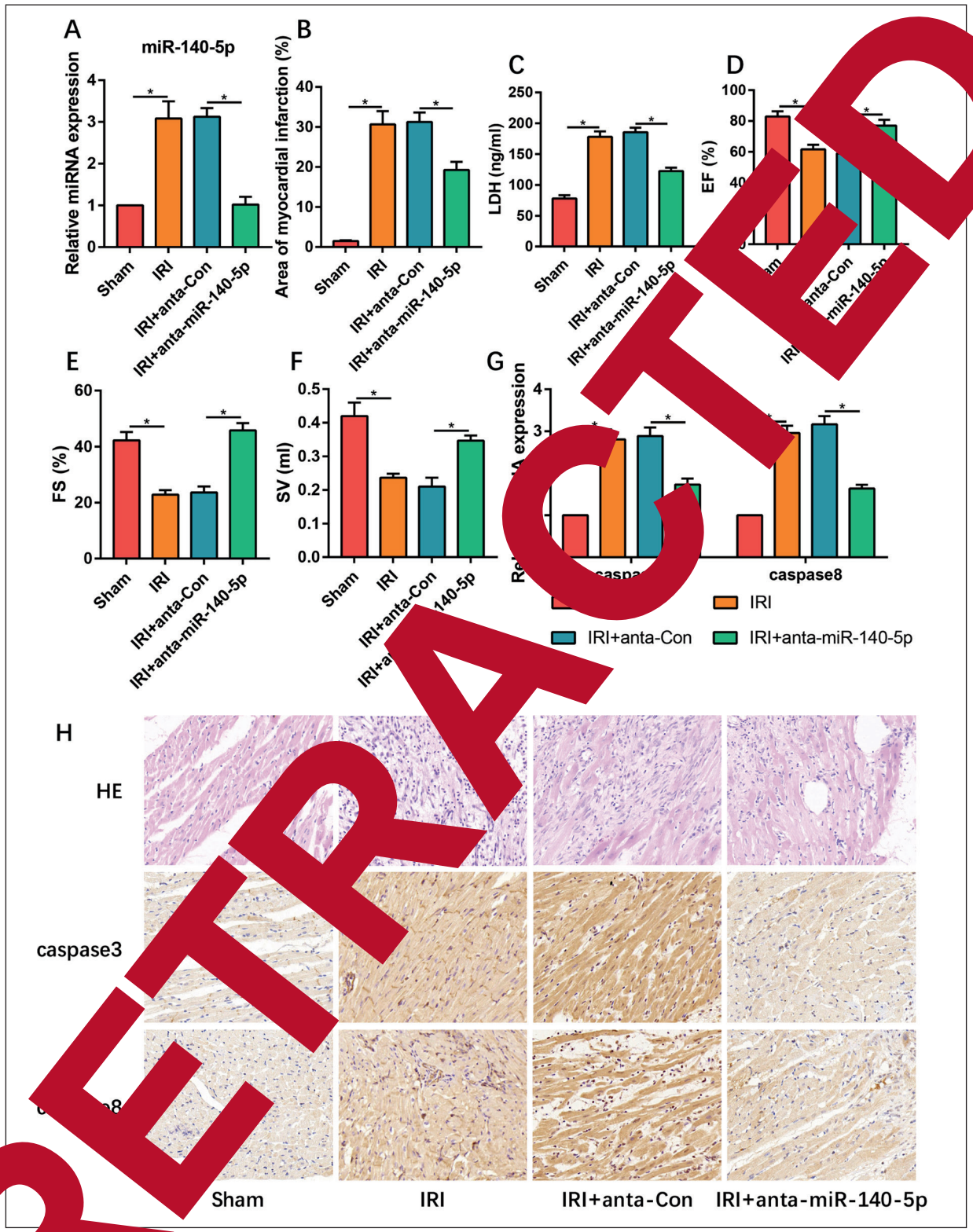

Figure 1. MiR-140-5p was highly expressed in myocardial tissue of IRI rats and anta-miR-140-5p can reduce myocardial IRI. **A,** The changes of miR140-5p expression in IRI rats. **B,** The area of myocardial infarction was detected by TTC staining. **C,** The concentration of LDH in rat serum. **D-F,** EF, FS and SV of rats was detected by echocardiography. **G,** mRNA expression of caspase-3/8 was detected by RT-PCR. **H,** HE staining and IHC staining of caspase3/8 (magnification: 200×). ("*" means the difference is statistically significant, $p<0.05$).

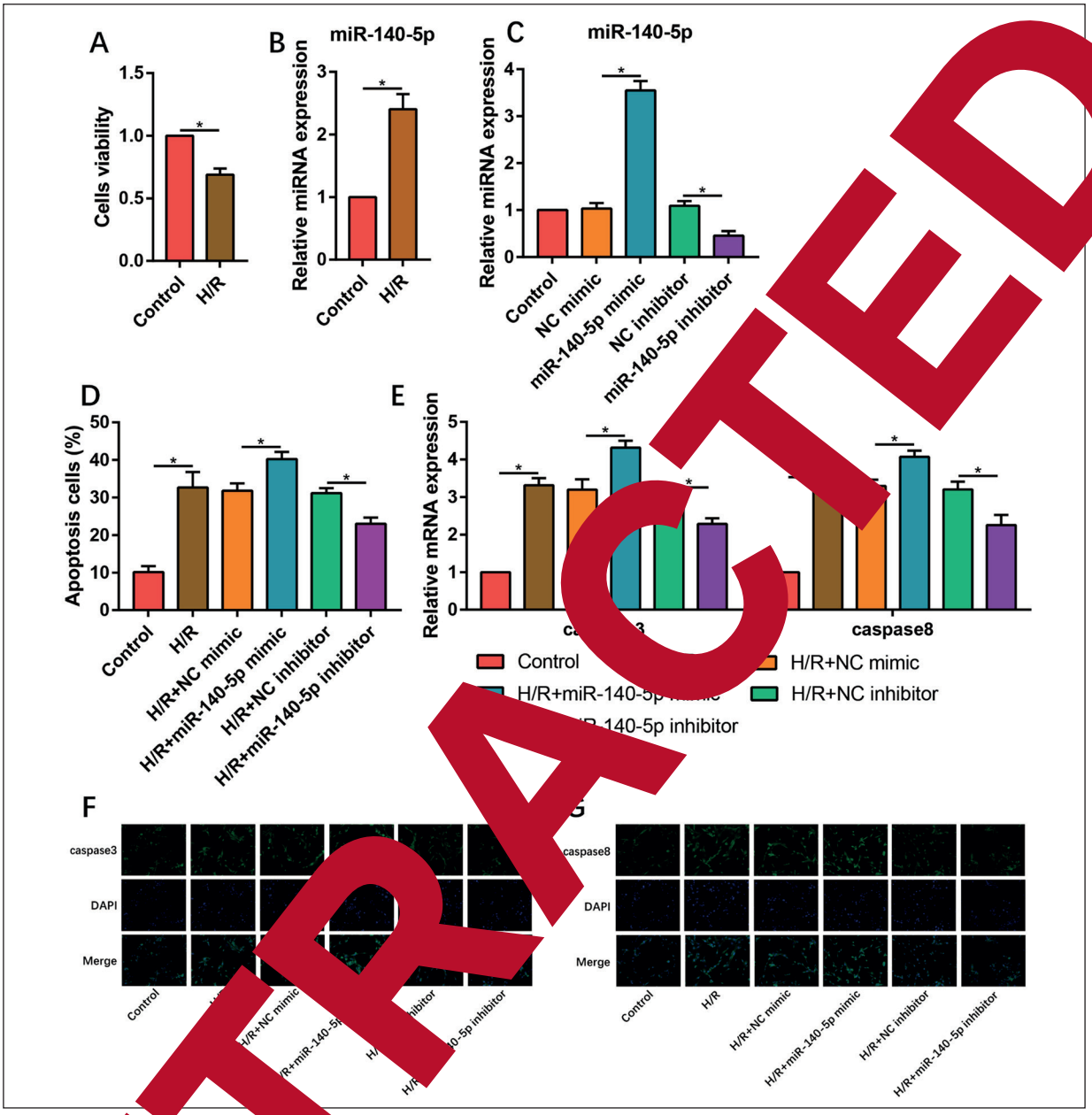

Figure 2. M 40-5p was highl ed in H/R-induced H9c2 cells and miR-140-5p inhibitor can reduce H/R-induced cell damage. A cells viability of H9c2 s was detected by CCK8 assay. **B-C,** The changes of miR140-5p expression in H9c2 cells. **D** apoptos ate of H9c2 cells was detected by flow cytometry. **E,** mRNA expression of caspase3/8 was detected by q R. **F-G** esults of caspase3/8 in H9c2 cells (magnification: 200×). ("*" means the difference is statistically sig $p<0$

uciferase assay to detect the interaction between miR-140-5p and BCL2L1. MiR-140 mimic and WT-BCL2L1-3'UTR were us H9c2 cells. The results showed after transfection of WT-BCL2L1-3'UTR, the l of luciferin in H9c2 cells was significantly while MUT-BCL2L1-3'UTR had no such ect (Figure 3B). In addition, the results of RT-PCR also showed that miR-140-5p can act on BCL2L1 and degrade it (Figure 3C).

Inhibition of BCL2L1 Attenuated the Protective Effect of MiR-140-5p Inhibitor on H9c2 Cells

To verify the effect of BCL2L1 in H9c2 cells, we used siRNA-BCL2L1 to reduce the expression

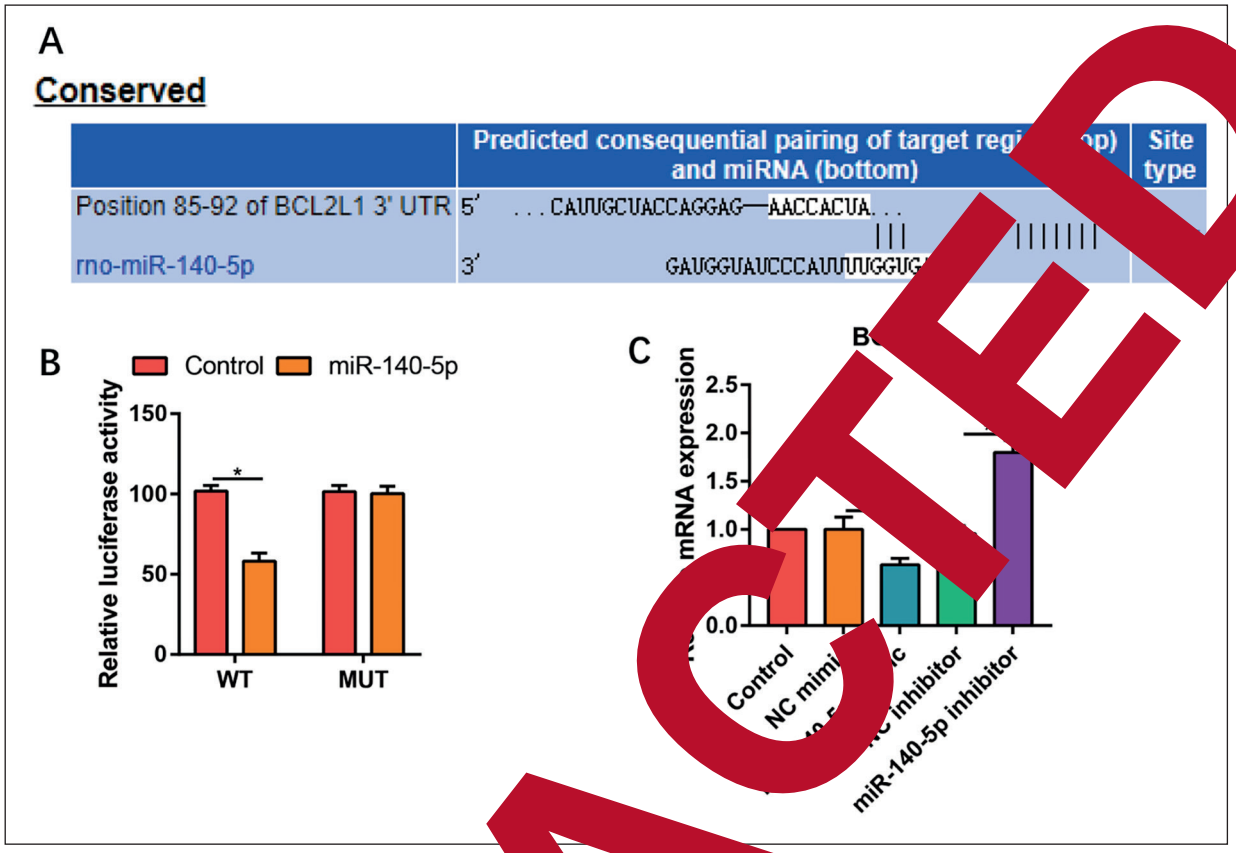

Figure 3. MiR-140-5p binds BCL2L1 and induces its degradation. **A,** MiR-140-5p was predicted to have a conserved binding site to BCL2L1. **B,** Dual-Luciferase reporter assay showed that miR-140-5p promoted the degradation of BCL2L1 mRNA. **C,** mRNA expression of BCL2L1 was detected by RT-PCR. (*means the difference is statistically significant, $p<0.05$).

of BCL2L1 in the cells [illegible] RT-PCR was used to verify its transfection efficiency. CCK-8 assay detected the viability of H9c2 cells. MiR-140-5p inhibitor partially restore IRI-induced decrease in cell viability, while siRNA-BCL2L1 inhibits the effect of miR-140-5p inhibitor (Figure 4B). Flow cytometry also showed that siRNA-BCL2L1 reduced the inhibitory effect of miR-140-5p inhibitor on apoptosis (Figure 4C). RT-PCR (Figure 4D) and IF staining (Figure 4E, 4F) detected the expression of caspase3/8 mRNA and protein in H9c2 cells respectively. We found that inhibition of BCL2L1 increased the expression of caspase3/8 mRNA and protein.

Discussion

Ischemia is a common clinical disease that can occur in many tissues and organs. Diseases caused by tissue ischemia are collectively referred to as ischemic diseases[12]. The main cause of myocardial ischemia is coronary artery stenosis, which generally exceeds 70%. Decreased myocardial blood flow perfusion at this time often induces myocardial hypoxia and causes metabolic disorders[13]. When the ischemic myocardium is reperfused, the myocardium is often damaged to different degrees, which induces arrhythmia and other symptoms. Severe myocardial IRI can even cause ventricular contraction and diastolic dysfunction, and cause myocardial cell necrosis, cardiomyocyte autophagy, and cardiomyocyte apoptosis[14]. MiRNA, as a medical research hotspot in recent years, has been found to be a therapeutic target for many diseases. In order to study the effect of miR-140-5p on myocardial IRI, we made a model of myocardial IRI using rats and detected the high expression of miR-140-5p in injured myocardial tissue. We determined the effect of IRI model by TTC staining and myocardial injury marker detection. The results showed that the myocardial infarction of the rats in the Sham group did not appear, while

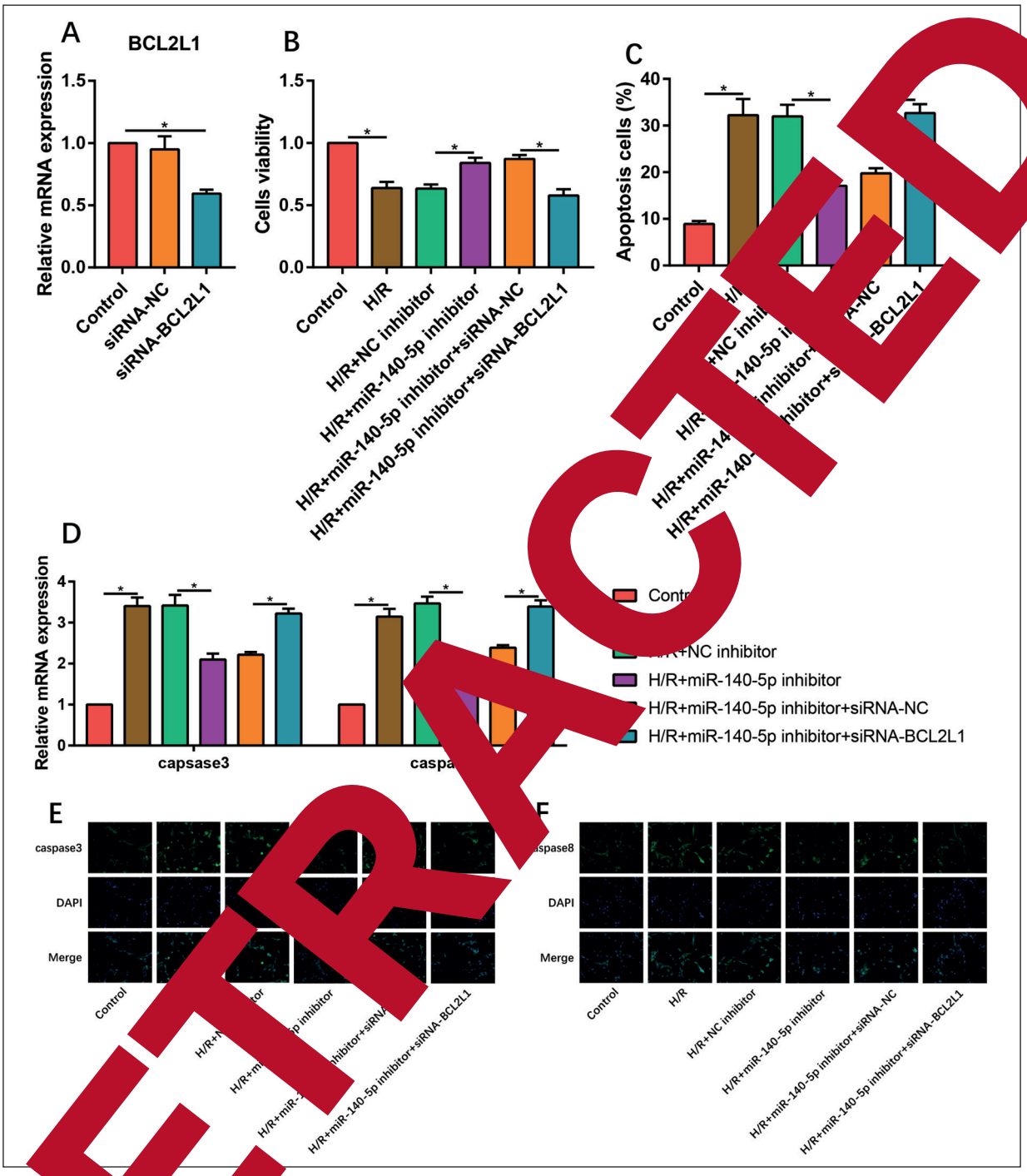

Figure tion of 2L1 attenuated the protective effect of miR-140-5p inhibitor on H9c2 cells. **A,** qRT-PCR ined t fec fficiency of siRNA-BCL2L. **B,** Cells viability of H9c2 cells was detected by CCK8 assay. **C,** the rate o was detected by flow cytometry. **D-F,** Expression of caspase3/8 was determined by qRT-PCR and IF st g (magni n: 200×). ("*" means the difference is statistically significant, $p<0.05$).

rea of myocardial infarction in the rats with ked coronary artery increased significantly, i g that the rat IRI model was successfully e lished. Compared with IRI group and IRI + anta-Con group, the area of myocardial infarction in anta-miR-140-5p treated rats was improved. In addition, the cardiac function test in rats also found that EF, FS, and SV in IRI rats

were significantly reduced, indicating that the contractile and diastolic functions of myocardium in IRI rats were decreased. After treating rats with anta-miR-140-5p, the EF, FS and SV of rats all increased, which also confirmed the myocardial protective effect of anta-miR-140-5p. In the experiments on pathological staining and IHC staining of rat myocardial tissue, we also found that myocardial injury and apoptosis in rats treated with anta-miR-140-5p were significantly improved. *In vitro* experiments, we make cell models of IRI by H/R. After H/R treatment, the proliferation level of H9c2 cells decreased significantly, indicating that H/R successfully induced damage to H9c2 cells. The expression of miR-140-5p in H/R-induced cells was significantly higher than that in the Control group. This is similar to the results of animal experiments. In addition, miR-140-5p inhibitor was found to reduce the apoptosis rate and apoptosis molecule (caspase3/8) in H9c2 cells. Caspase3 is the main terminal cleaving enzyme in the process of apoptosis. Caspase3 is activated in the early stages of apoptosis, and is the last known execution factor of apoptosis[15]. MiR-140-5p was ... to have possible binding sites with BCL2... the results of the Dual-Luciferase reporte... eriment also confirmed that miR-140-5p can ... and degrade BCL2L1 mRNA. The BCL2 ... mily also plays an important role in the proce... of apoptosis[16]. The BCL2 fam... ided into three different subfamilies ... rding ... the differences in function and s... ture, ar... which the BCL2 subfamily pl... role ... apoptosis, mainly co... ose... , BCL-xL, BCL-W, and BCL1... s a me... f the BCL2 family, BCL2L1 i... volved in th... lopment of many diseas... t al[18] studied ... senchymal stem ce... MSC... t showed a decrease in BCL2L1 under hea... s, leading to the apoptosis ... MSCS. They fo... at epigallocatechin-... late increased BCL2L1 and thus protects ... s from ... t stress. Ghaemi et al[19] also fou... t mi... 2 can i... uce glioblastoma cell apopt... nibitin... L2L1 and MCL1. To ... ify th... of B... L1 in cardiomyocytes, ... d siR... uce BCL2L1 expression in H9c... lls. The ... lts of CCK-8 and flow cytomet... vealed that after BCL2L1 was downregu... cells, the cell proliferation level ... eased and the apoptosis rate increased. This ... cates that BCL2L1 is a protective gene of ... lls. RT-PCR and IF staining also confirm... his. In the study of myocardial fibrosis, Schaefer[20] found that BCL2L1 plays an important role in stabilizing the mitochon... brane potential of cardiomyocytes ... pro... kinase CK2 can regulate the redo... lance in the cell by affecting the expressio... CL2L1, thereby protecting the myocardial ce... n oxidative stress.

MiR-140-5p was ori... y discover... cartilage-specific miR... in ze... fish. It ... miRNA that regul... carti... development and proliferation, a... nta... he hom... tasis of the cartilage ... lo... sion i... ated to the occurren... osteoa... [21]. ...R-140-5p expression i... uced in huma... ar smooth muscle c... l with seru... ee medium. This su... ts th... -140-5p may play a key role in vascular smo... scle phenotypic transfo... [22]. MiR-140-5p ... also regulate cell c... and cell proliferation. By targeting the tran... ption factor S... miR-140-5p can promote the ... liferation of ... ndrocytes and suppress the ... cycle[23]. In br... cancer, miR-140-5p inhibits t... urrence ... development of breast cancer by i... , SOX2 and SOX9 signaling pathways[24]. Xing et al[25] found that miR-140-5p can ... ggravate the damage of H9c2 cells by regulating ... addition, miR-140-5p is also involved ... the ... ccurrence and development of various inflammatory diseases. After myocardial injury induced by doxorubicin, miR-140-5p increased and then induced apoptosis of cardiomyocytes *via* regulating Nrf2 and VEGFA/14-3-3γ signaling pathways[26,27]. In a hypoxic-induced pulmonary hypertension model, upregulation of miR-140-5p promoted the apoptosis of pulmonary artery smooth muscle cells by regulating SOD2 and Dnmt1[28]. These results indicated that miR-140-5p plays an important role in the occurrence and development of multiple diseases. We also demonstrated the effect of miR-140-5p on cardiomyocytes in animal experiments and found another regulatory way for miR-140-5p. These results indicated that miR-140-5p can influence the process of myocardial IRI in various ways. Therefore, miR-140-5p may be a new target for the treatment of myocardial IRI.

To sum up, mir-140-5p, as an important regulatory factor regulating a variety of biological activities *in vivo*, has an important effect on myocardial IRI. To our knowledge, this is the first study to investigate the effect of miR-140-5p on myocardial IRI. We believed that this study can provide a new target and theoretical basis for the clinical treatment of myocardial IRI.

Conclusions

Altogether, this study showed that, in myocardial IRI, miR-140-5p can target the anti-apoptotic molecule BCL2L1 in cardiomyocytes, leading to the degradation of BCL2L1, thereby promoting the apoptosis of cardiomyocytes. Therefore, the inhibition of miR-140-5p can be used as a treatment for myocardial IRI.

Conflict of Interest

The Authors declare that they have no conflict of interests.

References

1) Mefford MT, Li BH, Qian L, Reading SR, Harrison TN, Scott RD, Cavendish JJ, Jacobsen SJ, Kanter MH, Woodward M, Reynolds K. Sex-specific trends in acute myocardial infarction within an integrated healthcare network, 2000 through 2014. Circulation 2020; 141: 509-519.

2) Chi HJ, Chen ML, Yang XC, Lin XM, Sun H, Zhao WS, Qi D, Dong JL, Cai J. Progress in thera... myocardial ischemia reperfusion injury. ... Targets 2017; 18: 1712-1721.

3) Yellon DM, Hausenloy DJ. Realizing the clinic... tential of ischemic preconditioning and postco... tioning. Nat Clin Pract Cardiovasc Med 2005; ... 568-575.

4) Krzywonos-Zawadzka A, Fr... wicki G, Wozniak M, Bil-Lula I. Multi... preve... or therapy of ischemia-reperf... injury ... heart-Mini-review. Environ ... Pharm... 55-59.

5) Ong SB, Katwadi... vek XY, ... NI, Chinda K, Ong SG, Hausen... J. Non-cod... As as therapeutic targe... preventing my... l ischemia-reperf... Expert Opin ... ner Targets 2018; ... 247-2...

6) Makhdo... P, Roohbakh... Karimi G. MicroRNAs ... ate mitochondria... otic pathway in my... ial ischemia-reperfus... n-injury. Biomed P... acothe... 16; 84: 1635-1644.

7) ... A, Ra... Orticell... M, Lucarelli M. The com... betwee... A methylation and miRNA ... e exp... on regulation. Biochimie 2020. ... 10... lochi.2020.02.006.

... quinos... S, Genschel C, Viereck J, Rump ... yongyosi I... axler D, Riesenhuber M, Spannbau... Lukovic D, Weber N, Zlabinger K, Hasimbegovic ... iedler J, Dangwal S, Fischer M, de la ... oche J, ... ojciechowski D, Kraft T, Garamvolgyi R, Neitzel S, Chatterjee S, Yin X, Bar C, Mayr M, Xiao ... Thum T. Preclinical development of a miR-132 ... itor for heart failure treatment. Nat Commun ... 0; 11: 633.

9) Duale N, Eide DM, Amberger ML, Graupner A, Brede DA, Olsen AK. Using predicti... to identify miRNA-based markers ... rate chronic stress. Sci Total En... 2020; 7... 137068.

10) Xue J, Zhang Z, Li X, Ren ... g Q. Long non-coding RNA TTN-AS1 prom... ast cancer cell migration and inv... n via sp... miR-140-5p. Oncol Lett 202... : 1255-126...

11) Oses M, Margareto ... ortillo ... R, Aguiler... Labayen I. Circulat... miRNAs ... biomarkers of obesity and ob... ssoci... comorb... ties in children and ... odo... ystema... eview. Nutrients 20... t: 28...

12) Xia H, Liu ... ng W, Zeng ... en P, Zhong Z, Ye Q... nerve stimulat... viates hepatic isch... eperfusion inj... by regulating glut... e p... n and transformation. Oxid Med Cell Longev... 2020: 1079129.

13) ... , Heusch G, C... Van de Werf F. Evolving therapies for myoc... dial ischemia/reperfusion injury. J Am Coll Cardiol 2015; 65: 1454-1471.

... Aldiwani H, Za... , Suppogu N, Quesada O, Johnson ... D, Mehta PK... felt C, Petersen J, Azarbal B, Sam... B, And... RD, Shaw LJ, Kar S, Handberg E, ... CJ, Bairey MC. Angina hospitalization ... n women with signs and symptoms of ischemia but no obstructive coronary artery dis... ase: a report from the WISE (Women's Ischemia ... me Evaluation) Study. J Am Heart Assoc ... ; 9: e13168.

15) Gupta S, Knowlton AA. HSP60, Bax, apoptosis and the heart. J Cell Mol Med 2005; 9: 51-58.

16) Vogler M, Walter HS, Dyer M. Targeting anti-apoptotic BCL2 family proteins in haematological malignancies - from pathogenesis to treatment. Br J Haematol 2017; 178: 364-379.

17) Polcic P, Mentel M. Reconstituting the mammalian apoptotic switch in yeast. Genes (Basel) 2020; 11: 145.

18) Butt H, Mehmood A, Ejaz A, Humayun S, Riazuddin S. Epigallocatechin-3-gallate protects Wharton's jelly derived mesenchymal stem cells against in vitro heat stress. Eur J Pharmacol 2020; 872: 172958.

19) Ghaemi S, Arefian E, Rezazadeh VR, Soleimani M, Moradimotlagh A, Jamshidi AF. Inhibiting the expression of anti-apoptotic genes BCL2L1 and MCL1, and apoptosis induction in glioblastoma cells by microRNA-342. Biomed Pharmacother 2020; 121: 109641.

20) Schaefer S, Guerra B. Protein kinase CK2 regulates redox homeostasis through NF-κB and Bcl-xL in cardiomyoblasts. Mol Cell Biochem 2017; 436: 137-150.

21) Papathanasiou I, Balis C, Trachana V, Mourmoura E, Tsezou A. The synergistic function of miR-140-5p and miR-146a on TLR4-mediated cytokine secretion in osteoarthritic chondrocytes. Biochem Biophys Res Commun 2020; 522: 783-791.

22) Zhu TT, Zhang WF, Yin YL, Liu YH, Song P, Xu J, Zhang MX, Li P. MicroRNA-140-5p targeting tumor necrosis factor-alpha prevents pulmonary arterial hypertension. J Cell Physiol 2019; 234: 9535-9550.

23) Wang Y, Shen S, Li Z, Li W, Weng X. MIR-140-5p affects chondrocyte proliferation, apoptosis, and inflammation by targeting HMGB1 in osteoarthritis. Inflamm Res 2020; 69: 63-73.

24) Bai F, Yu Z, Gao X, Gong J, Fan L, Liu F. Simvastatin induces breast cancer cell death through oxidative stress up-regulating miR-140-5p. Aging (Albany NY) 2019; 11: 3198-3219.

25) Xing B, Li QJ, Li H, Chen SS, Cui ZY, Ma J, Zhang ZW. MiR-140-5p aggravates hypoxia-induced cell injury via regulating MLK3 in H9c2 cells. Biomed Pharmacother 2018; 103: 1652-1657.

26) Chen XY, Huang WL, Peng XP, Lv YN, Li JH, Xiong JP. MiR-140-5p mediates bevacizum[illegible] cytotoxicity to cardiomyocytes by[illegible] VEGFA/14-3-3gamma signal p[illegible]ay. Toxic Res (Camb) 2019; 8: 875-884.

27) Zhao L, Qi Y, Xu L, Tao X, Han [illegible] Peng J. MicroRNA-140-5p aggravates doxo[illegible]-induced cardiotoxicity by promot[illegible]myocard[illegible]lativ stress via targeting N[illegible]nd Sirt2. Re[illegible] 2018; 15: 284-296.

28) Zhang Y, Xu J. Mi[illegible]-5p re[illegible]es hypoxia-mediated human p[illegible]ry a[illegible] smoot[illegible]uscle cell proliferati[illegible] ap[illegible]d differ[illegible]tion by targeting D[illegible] and [illegible]ing S[illegible] expression. Bioc[illegible] Biophys Re[illegible] 2016; 473: 342-348.